



1 **Design and evaluation of BOOGIE: a collector for the analysis**
2 **of cloud composition and processes: Biological, Organics,**
3 **Oxidants, soluble Gases, inorganic Ions and metal Elements**
4

5 Mickael Vaitilingom^{1,2*}, Christophe Bernard³, Mickaël Ribeiro^{1,3}, Christophe Berthod⁴,
6 Angelica Bianco¹, Laurent Deguillaume^{1,3*}

7
8 ¹ Laboratoire de Météorologie Physique, UMR 6016, CNRS, Université Clermont Auvergne, 63178 Aubière,
9 France

10 ² Laboratoire de Recherche en Géosciences et Énergies, EA 4539, Université des Antilles, 97110 Pointe-à-Pitre,
11 France

12 ³ Observatoire de Physique du Globe de Clermont-Ferrand, UAR 833, CNRS, Université Clermont Auvergne,
13 63178 Aubière, France

14 ⁴ Division Technique de l'Institut National des Sciences de l'Univers, UAR 855, CNRS, 91190 Gif-sur-Yvette,
15 France.

16
17 *Correspondence to:* Laurent Deguillaume (laurent.deguillaume@uca.fr) and Mickael Vaitilingom
18 (mickael.vaitilingom@univ-antilles.fr)

19
20 **Abstract.** Cloud/fog droplets comprise a myriad of chemical compounds and are living environments in which
21 microorganisms are present and active. These chemical and biological elements can evolve in various ways within
22 the cloud system, and the aqueous transformation of chemicals contributes to atmospheric chemistry. In situ cloud
23 studies are fundamental in this sense, because they enable us to study the variability in cloud chemical composition
24 as a function of environmental conditions and assess their potential for transforming chemical compounds. To
25 achieve this objective, cloud water collectors have been developed in recent decades to recover water from clouds
26 and fogs using different designs and collection methods. In this study, a new active ground-based cloud collector
27 was developed and tested for sampling cloud water to assess the cloud microbiology and chemistry. This new
28 instrument, BOOGIE, is an easy mobile sampler for cloud water collection with the objective of being cleanable
29 and sterilisable, respecting chemical and microbial cloud integrity, and presenting an efficient collection rate of
30 cloud water. Computational fluid dynamics simulations were performed to theoretically assess the capture of cloud
31 droplets by this new sampler. Few turbulences have been observed inside the collector and a 50% collection
32 efficiency cutoff of 10 μm has been estimated. The collector was deployed at Puy de Dôme station under cloudy
33 conditions for evaluation. The water collection rates were measured at $156 \pm 52 \text{ mL h}^{-1}$ for a collection of 17 cloud
34 events; considering the measured liquid water content, the sampling efficiency of this new collector has been
35 estimated at $87.2 \pm 8.6\%$ over the same set of cloud events. BOOGIE was compared with other active cloud
36 collectors commonly used by the scientific community (Cloud Water Sampler and Caltech Active Strand Cloud
37 Collector version 2). Four cloud events were collected; the three samplers presented similar collection efficiencies
38 (between 79% and 88% on average). The measured ionic composition was comparable even if differences were
39 highlighted between collectors, the consequence of different designs, and the intrinsic homogeneity in the chemical
40 composition within the cloud system.

41
42 **Keywords:** Cloud chemistry, monitoring, cloud water collector, chemical composition, biological composition.
43



44 1 Introduction

45 The chemical composition of clouds is highly complex because it results from various processes: (1) the mass
46 transfer of soluble compounds from the gas phase into cloud droplets, (2) dissolution of the cloud condensation
47 nuclei released into the aqueous phase as a complex mixture of soluble molecules, and (3) photochemical and
48 biological transformations leading to new chemical products (Herrmann et al., 2015).

49 Field experiments to characterise this multiphasic medium were developed in the 1950s but increased in the 1980s
50 because of precipitation acidification through sulphur oxidation in cloud droplets (Munger et al., 1983; Hoffmann,
51 1986; Kagawa et al., 2021). These studies have highlighted that cloud and fog processing is efficient and plays a
52 major role in air pollution by transforming gases and aerosol particles. Numerous investigations have focused on
53 inorganic compounds that control aqueous-phase acidity (Pye et al., 2020). The production of strong acids has
54 been assessed because it increases particle mass when clouds/fogs evaporate and leads to acidic deposition when
55 clouds precipitate (Tilgner et al., 2021). Early in the 1990s and much more so in the 2000s, researchers investigated
56 the composition of dissolved organic matter in cloud/fog water which has multiple natural and anthropogenic
57 sources of primary or secondary origins (Herckes et al., 2013). Based on scientific issues, specific classes of
58 compounds have been targeted, such as short-chain carboxylic acids and carbonyls (Löflund et al., 2002; Munger
59 et al., 1995; Sun et al., 2016) and more recently carbohydrates and amino acids (Triesch et al., 2021; Renard et al.,
60 2022). Attention has also been paid to the detection of pollutants with strong sanitary effects, such as HAP,
61 phenols, and phthalates (Lüttke et al., 1999; Li et al., 2010; Lebedev et al., 2018; Ehrenhauser et al., 2012) because
62 they can impact ecosystems through precipitation (Wright et al., 2018). Recent investigations using high-resolution
63 mass spectrometry have revealed the complexity of the organic matrix, with thousands of detected molecules (Zhao
64 et al., 2013; Cook et al., 2017; Bianco et al., 2018; Sun et al., 2021). This organic matter is processed during the
65 cloud lifetime and has raised new scientific questions such as the formation of secondary organic aerosol by
66 aqueous phase reactivity (“aqSOA”) (Blando and Turpin, 2000; Lamkaddam et al., 2021) and light absorbing
67 material referring to brown carbon (“BrC”) (Laskin et al., 2015). Microorganisms are also present and active in
68 cloud droplets (Amato et al., 2005; Vätilingom et al., 2012; Xu et al., 2017; Hu et al., 2018). They can be
69 incorporated because they serve as cloud condensation nuclei (Bauer et al., 2002; Deguillaume et al., 2008) and
70 can impact cloud water composition through their metabolism by consuming or producing new molecules (Liu et
71 al., 2023; Vätilingom et al., 2013; Pailler et al., 2023). Many investigations have focused on biological cloud
72 characterisation (Amato et al., 2017; Wei et al., 2017).

73 Monitoring cloud chemical and biological compositions is crucial for evaluating the role of key environmental
74 parameters such as emission sources, atmospheric transport and transformations, and physicochemical cloud
75 properties such as cloud acidity or microphysical cloud properties (liquid water content [LWC] and size
76 distribution of cloud droplets). Specific sites or aircraft campaigns allow the collection of cloud water influenced
77 by marine (Macdonald et al., 2018; Gioda et al., 2011), continental (Van pinxteren et al., 2016; Hutchings et al.,
78 2009; Lawrence et al., 2023; Van Pinxteren et al., 2014) and urban emissions (Li et al., 2020; Guo et al., 2012;
79 Herckes et al., 2002) over various continents (mainly Europe, North America, Asia). Owing to their poor
80 accessibility and remoteness, certain geographical locations have been less investigated, such as the Arctic region
81 (Adachi et al., 2022), tropical environments (Dominutti et al., 2022), or marine surfaces (Van Pinxteren et al.,
82 2020). Field experiments combining cloud water and gaseous phase chemical characterisation have also been



83 conducted to evaluate the partitioning of molecules between these two phases and whether bulk cloud water obeys
84 Henry's law (Van Pinxteren et al., 2005; Wang et al., 2020). Bulk aqueous cloud media are used for laboratory
85 investigations to study the aqueous transformations induced by light and the presence of microorganisms
86 (Schurman et al., 2018; Bianco et al., 2019).

87 Therefore, the scientific community requires regular and long-term measurements of cloud chemical and biological
88 parameters. However, cloud sampling procedures are challenging. In recent decades, different samplers have been
89 developed and deployed in the field, which can be operated under specific environmental conditions and present
90 different collection efficiencies possibly impacted by meteorological conditions. These are commonly based on
91 the impact of cloud droplets on the collector surface and avoid the collection of small droplets (<5 µm in diameter).
92 Their collection efficiency and 50% collection cutoff diameter (d₅₀) were calculated and estimated to evaluate the
93 accuracy of droplet collection by the sampler. Monitoring of the microphysical cloud properties (LWC and size
94 distribution) is required to assess this. These samplers refer to "bulk" cloud water collectors because they group
95 droplets of different sizes. Many types of collectors can be listed: active or passive ground- or aircraft-based, and
96 single- or multi-stage. Passive collectors are dependent on wind speed because the air needs to flow through them,
97 allowing sampling. Active collectors are ground-based collectors through which air-containing droplets are forced
98 to flow inside the system by devices such as pumps or ventilator fans. They have been designed and commonly
99 used to obtain higher volumes of water required for laboratory investigations. Ground-based samplers are easy to
100 install, inexpensive, and suitable for long-term observations. Samplers installed on aircrafts are less widely used,
101 and recent developments by Crosbie et al. presenting a new axial cyclone cloud water collector have shown to
102 strongly improve the collection efficiency of cloud droplets compared to previous samplers (Crosbie et al., 2018).
103 All these samplers are described in reviews where and their designs, their advantages, and limitations are presented
104 (Roman et al., 2013; Skarżyńska et al., 2006).

105 Two types of ground-based active samplers are often used by the scientific community to monitor cloud chemistry
106 and microbiology: the Cloud Water Sampler (CWS) from Vienna University (Kruisz et al., 1993) and the Caltech
107 Active Strand Cloudwater Collector (CASCC) from Caltech University (Daube et al., 1987; Demoz et al., 1996;
108 Collett Jr et al., 1990). These collectors have been adapted for long-term monitoring (Gioda et al., 2013; Guo et
109 al., 2012; Deguillaume et al., 2014; Renard et al., 2020) and specific field campaigns (Wieprecht et al., 2005;
110 Van pinxteren et al., 2016; Li et al., 2017; Li et al., 2020; Bauer et al., 2002).

111 The Puy de Dôme (PUY) station is a reference site for the collection of cloud water from samples collected between
112 2001 and the present. The sampler was obtained from Kruisz et al. (1993) and has been widely used for microbial
113 and chemical atmospheric studies at this site (Marinoni et al., 2004; Marinoni et al., 2011; Bianco et al., 2017; Joly
114 et al., 2014) This model can collect wet or supercooled droplets, even at high wind speeds. It is made of aluminium
115 or Teflon; the collection vessel can be removed for sterilisation and cleaning. However, the collected water volume
116 of 10–60 mL per hour is a limit for chemical and microbial analyses that require increasing volumes. For long
117 collection times, the vessel should be removed regularly to transfer the water into a sterile storage bottle. These
118 manipulations expose the samples to contamination. The aspiration system must be powerful and, consequently,
119 heavy and energy-consuming, which limits mobile sampling. The objective of this study was to present a new
120 ground-based cloud collector that responds to different constraints. This tool should be suitable for analysing cloud
121 microbiology and chemistry, easy to clean and sterilise, allow the collection of high volumes of water, and be easy



122 to deploy for field campaigns (light and low energy consumption). To achieve these objectives, we developed a
123 BOOGIE collector. This study describes this instrument and compares it to other commonly used samplers to
124 evaluate its efficiency.

125 **2 Materials and Methods**

126 **2.1 Conception of the BOOGIE cloud collector**

127 The 3D drawing was performed with Autodesk® Inventor 2016 and recently updated using the 2019 version. The
128 prototype of the collector used in this study was fabricated on an aluminium stand (Al 5754 and 6060). This
129 material exhibits robust properties and can be easily sterilised by autoclaving before field collection. Aluminium
130 plates were cut using a laser and folded using a metal press. The collection funnel was adapted to a GL 45 thread
131 to directly screw borosilicate glass or polytetrafluoroethylene (PTFE) bottles. All the aluminium parts were treated
132 by QUANALOD® anodisation, with thickness of 20 µm, suitable for aluminium objects exposed to harsh
133 environmental conditions. All parts were thoroughly cleaned to eliminate all manufacturing residue and several
134 cycles of sterilisation by autoclaving (121°, 20 min per cycle) were performed to clean the collector.

135 The vacuum inside the collector was ensured by an axial fan (EMB-papst®, model 6300TD, S-Force, 40 W, 12 V
136 DC) able to work under wet conditions and temperatures of -20 °C to 70 °C. It has a fan diameter of 172 mm and
137 a maximum flow capacity of 600 m³ h⁻¹ (manufacturer data). It is equipped with a controlled voltage for speed
138 setting, which allows modulation of the fan velocity according to 10 increasing intensities. To measure the air inlet
139 and outlet velocity, a thermal anemometer efficient from 0.2 to 20 m s⁻¹ was used (model Lutron AM-4204 from
140 RS PRO®).

141 **2.2. Computational Fluid dynamics (CFD) simulations**

142 Finite element modelling and simulations were performed using Simcenter 3D software from Siemens Industry
143 Software Inc., version 2022.1. The solver environment was Simcenter 3D Thermal/Flow Advanced Flow. The
144 flow and particle tracking solvers are proprietary to Maya Heat Transfer Technologies. Other numerical
145 computations and figures were performed using MATLAB version 2021a.

146 The fluid domain is represented by the inner volume of the collector. To compute a realistic flow inside the
147 collector, it is necessary to consider the structure of the collector, which is composed of thin walls and metal plates,
148 to enable air deflection and the collection of cloud water droplets. The Simcenter 3D software allows the generation
149 of a volume or mesh directly from the boundaries of different parts of the collector; however, this method was
150 unsuitable because of the thin inner walls. The fluid domain was built using successive Boolean subtractions by
151 leaving a void in the right place, leading to a realistic geometry of the air volume (**Figure S1a**).

152 A finite element mesh was created using CTETRA4 solid elements. The element size was variable: the internal
153 mesh size was set to 20 mm, whereas the element size was set to 24 mm on the rear faces next to the fan and to
154 only 4 mm on the front face, allowing air deflection and the collection of droplets (**Figure S1b**). The total numbers
155 of elements and nodes were 869 799 and 178 610, respectively.

156 For the air inlet flow, three slots of the collector front face were defined as the inlet flow boundary conditions. The
157 flow direction was perpendicular to the front face and the external absolute pressure was equal to the ambient



158 pressure. For the air outlet flow, air velocity was applied to the rear circular face representing the fan. The
159 magnitude varied according to the velocity ranges. The vector was perpendicular to the face.

160 The fluid is the standard air at the altitude of 1500 m (*i.e.*, summit of the PUY), at 15 °C, with the following
161 physical characteristics: 1.1 kg m⁻³ for the mass density and 1.75 kg m⁻¹ s⁻¹ for the dynamic viscosity.

162 The outlet velocity of the fan can be modulated among 10 intensities. The resulting air inlet volume flows have
163 been measured using a hot-wire anemometer located in front of the slots. The surface area of the fan outlet was
164 17671 mm², and the total area of the three inlet slots was 11088 mm². Therefore, there was a theoretical ratio of
165 1.6 between the air inlet volume flow and the air outlet volume flows. To agree with the measured air inlet volume
166 flow, the outlet velocities for the collector simulations were varied for the CFD simulations between 1 and 10 m
167 s⁻¹ in 1 m s⁻¹ step.

168 Different particles were used in the simulation. The water drops were injected into the flow at the three air-inlet
169 slots. Eight different values of drop diameter were selected between 5 and 20 µm. The water droplets were
170 considered spherical. The drag coefficient was automatically calculated using the Reynolds number. The density
171 of water was assumed to be 1 kg/dm³. Gravity was applied to the cloud particles, and the gravity vector was defined
172 as the -Z axis with an acceleration amplitude of 9.81 m s⁻². The sizes and masses of each particle class are
173 summarised in **Table S1**.

174 In the air flow inside the collector, three vertical plates participated in droplet collection. If cloud water drops
175 impact them, they should flow to the bottom of the funnel. Therefore, there is a specific surface configuration; if
176 the water drops stick to the collection face, they do not rebound.

177 We selected the fully coupled pressure-velocity solver to solve the mass and momentum equations simultaneously
178 for each time step. The solver iterates the pressure and velocity solutions until convergence is achieved at each
179 time step. Modelling fluid flow turbulence is crucial for accurately simulating airflow. The flow solver uses
180 different turbulence models that add a viscosity term to the Navier–Stokes governing equations. The two-equation
181 model computes the viscosity term using two additional equations that are solved in parallel with the Navier–
182 Stokes equations. Among the two-equation models, the k-omega model was selected for this study. The steady
183 state time step was fixed to 0.01 s for all the model simulations.

184 For the steady-state simulation, the flow was fully developed, and its properties (velocity, pressure, and turbulence)
185 were used in the particle-tracking equation. During the analysis, the software solved the equation of motion for
186 each particle once per time step. Notably, because the particle tracking simulation is independent of the flow
187 simulation, the particles do not affect the 3D flow. The injection duration in the fluid domain was 60 s, which is a
188 good compromise between the relevant calculation and a reasonable simulation time.

189 **2.3 Experiments: inter-comparison of samplers**

190 **2.3.1 Sampling site**

191 The testing site of the different cloud collectors was the observatory of the PUY summit at 1465 m above sea level.
192 It is part of the Cézeaux-Aulnat-Opme-Puy De Dôme (CO-PDD) instrument platform for atmospheric research
193 (Baray et al., 2020). PUY is recognised as a global station in the Global Atmosphere Watch (GAW) network and
194 is part of the European and national research infrastructures Aerosol Cloud and Trace Gases Research



195 Infrastructure (ACTRIS) and the Integrated Carbon Observing System (ICOS). The PUY is often located in the
196 free troposphere, particularly during cloud events, and the characterised air is representative of synoptic-scale
197 atmospheric composition. Various biological, physical, chemical, and cloud microphysical parameters were
198 monitored on-site. For cloud microphysical properties, we use a ground-based scattering laser spectrophotometer
199 for cloud droplet volume measurements from Gerber Scientific, Inc. (Reston, VA, USA). All cloud microbiology
200 and chemistry data are available in the PUYCLOUD database ([https://www.opgc.fr/data-
201 center/public/data/puyccloud](https://www.opgc.fr/data-center/public/data/puyccloud)).

202 **2.3.2 Cloud collectors**

203 Two bulk cloud collectors were compared with a newly developed BOOGIE collector. These are active ground-
204 based collectors commonly used in cloud field studies. They have different collection efficiencies, resulting in
205 different volumes of cloud water that can be sampled. Cloud water collectors are generally designed to avoid the
206 particles below 5 microns to avoid sampling the interstitial aerosol around the droplets. This is a compromise to
207 obtain a sufficient volume of water with less contamination from dry and deliquescent particles. Typically, the
208 smallest droplets were not sampled. The 50% collection efficiency cutoff, based on the droplet diameter, is often
209 predicted from the impaction theory and strongly depends on the aerodynamic design of the impactor and the air
210 flow rate (Berner, 1988; Schell et al., 1992). The collection efficiency for in situ conditions will depend on the
211 LWC, and the meteorological conditions could strongly perturb the way the collectors are able to impact cloud
212 droplets.

213 *Caltech Active Strand Cloud water Collector: CASCC2*

214 A compact version of the original CASCC collector was used and lent by the Institut de Radioprotection et de
215 Sûreté Nucléaire (IRSN). This sampler, named CASCC2, was constructed according to the recommendations of
216 Demoz et al. (1996). It has an estimated cutoff diameter of 3.5 μm (droplet diameter collected with 50% collection
217 efficiency). The airflow passed through a set of six rows of stainless-steel strings (diameter, 0.5 mm) with a
218 velocity of 8.6 m s^{-1} . The strings were vertically tilted 35°. The collector design has been shown to generate a
219 stable airflow inside of 348 $\text{m}^3 \text{h}^{-1}$. The fraction of air sampled was calculated to be 86% (*i.e.*, 299 $\text{m}^3 \text{h}^{-1}$). The
220 volume fraction of the ambient droplet distribution collected was evaluated in Demoz et al. (1996), who showed
221 that this fraction is close to one over most of the LWC range (superior to 95% $>0.1 \text{ g m}^{-3}$ of LWC). Therefore, we
222 can estimate at the end a resulting sampled airflow at 284 $\text{m}^3 \text{h}^{-1}$ (4.73 $\text{m}^3 \text{min}^{-1}$). Cloud droplets coalesce on the
223 strands and fall into a bottle through a Teflon tube owing to the combination of gravity and aerodynamic resistance.
224 A description of the sampler is provided in **Figure S2**.

225 The collector body was stainless steel, the inlet contained the impaction rows, and the sample drainage was
226 removed before each sampling for cleaning and sterilisation. A sterilised amber glass bottle was placed under the
227 sample drainage during collection. This cloud collector was not adapted for temperatures $<0 \text{ }^\circ\text{C}$ because droplets
228 freeze upon impaction on metallic strains.

229 *Cloud Water Sampler: CWS*

230 This collector (**Figure S3**) was developed specifically to collect warm and supercooled clouds, which can either
231 freeze upon impaction or be collected directly in the liquid phase (Kruisz et al., 1993; Brantner et al., 1994). It was
232 designed to sample cloud water for specific studies on the detection for example of fungal spores and bacteria in



233 cloud water (Tenberken-Pötzsch et al., 2000; Bauer et al., 2002). It comprises a single-stage impactor backed by a
234 large wind shield (50 cm wide and 50 cm high) installed in front of the wind. The wind velocities were reduced in
235 front of the shield, and the flow was directed into the single-slit nozzle. Cloud droplets ranging up to 100 μm in
236 diameter were estimated to be stopped in front of the shield, stay airborne, and were sampled from a stagnant flow.
237 Cloud droplets, which were drawn through a slit 25 cm long and 1.5 cm wide, collided on a rectangular aluminium
238 collection plate installed horizontally, and water was collected in a reservoir below the plate. This sampler model
239 presents an estimated cutoff diameter at 50% collection efficiency of 7 μm at a sampling rate of 86 $\text{m}^3 \text{h}^{-1}$, as
240 indicated in Brantner et al. (1994). The CWS used at the PUY was a homemade collector following the
241 recommendation formulated by Krusiz et al. (1993); however, the suction system presented its own characteristics,
242 with an inlet air velocity of 13.5 m s^{-1} .

243 The blower was placed under the sampler and connected to the collector body via tubing. This was built of
244 aluminium, and the collection plate and vessel were removable for cleaning and sterilisation. In contrast to the
245 CASCC2, in which the water sample flowed into a glass bottle, in the CWS, the water remained in the collection
246 vessel during the sampling period. It is not possible to check the collected volume during sampling, and the water
247 must be regularly removed by opening the collector and transferring it to a storage bottle. This collector has been
248 used for studies at PUY since the 2000s (Marinoni et al., 2004) because the collection plate and vessel can be
249 sterilised in the laboratory, allowing for microbial analysis of cloud waters.

250 **2.3.4 Chemical and microbial analysis**

251 Chemical and biological analyses were performed on the cloud samples following the standardised procedures
252 described in Deguillaume et al. (2014). The main ions (Cl^- , NO_3^- , NH_4^+ , SO_4^{2-} , Na^+ , Ca^+ , Mg^+ , K^+) were analysed
253 using ion chromatography. Formaldehyde and hydrogen peroxide levels were measured using derivatisation
254 methods and analysed by fluorimetry. Total microbial cell counts, including bacterial, yeast, and fungal spores,
255 were determined using flow cytometry. The microbial energetic state was determined by measuring ATP and ADP
256 concentrations using bioluminescence. More information has been added to this analysis in the Supplementary
257 Information.

258 **2.3.5 Back-trajectory analysis**

259 The CAT model (Baray et al., 2020) was used to estimate the air mass history reaching the summit of the PUY
260 Mountain during the cloud-sampling period. This model uses the ECMWF ERA-5 wind fields and integrates a
261 topography matrix; back trajectories were calculated every hour during cloud sampling; the temporal resolution
262 was 15 min, and the total duration was 72 h. These calculations are fully described by Renard et al. (2020).

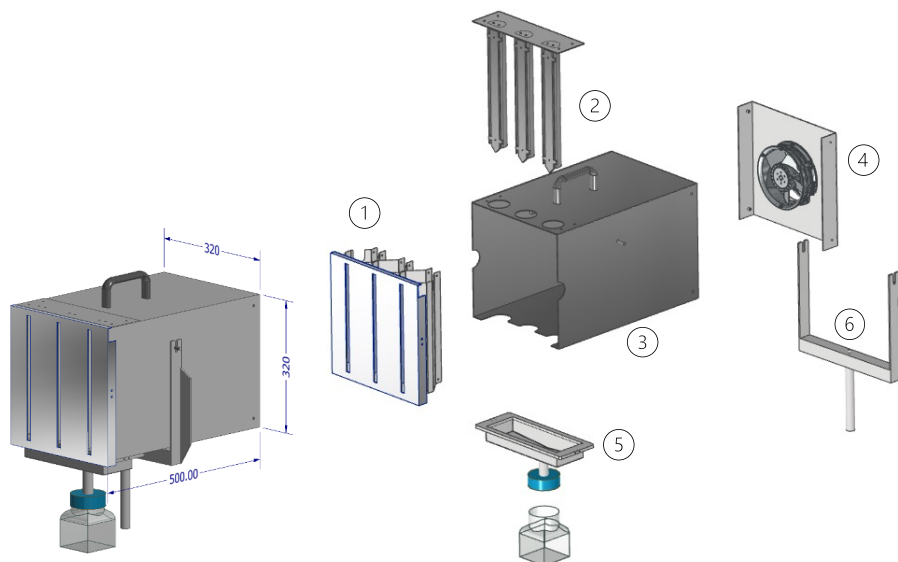
263 **3 Results**

264 **3.1. Conception and operating principles of the BOOGIE collector**

265 The new collector is a single-stage collector that uses impaction to sample the cloud droplets (Marple and Willeke,
266 1976). The collector is designed as a slit impactor. **Figure 1** shows the assembled collector (left) and the different
267 parts of the collector and how they should be assembled for sampling. A GIF animation (**Movie 1**) showing the
268 assembly of the collector before sampling is provided in the Supplementary Information. A photograph of the



269 collector is shown in **Figure S4**, and all the dimensions are detailed in **Figure S5**. Parts 1, 2, and 5 were sterilised
270 by autoclaving before sampling to allow for biological analysis.



271
272 **Figure 1. Schematic of the design of the BOOGIE collector. Assembly of the different parts of the BOOGIE collector:**
273 **(1) front face with the three slots; (2) impactation plates; (3) collector body; (4) rear face with the fan; (5) funnel; (6)**
274 **instrument holder.**

275 The cloudy air entered via three rectangular inlets oriented vertically side by side, each 30 cm long and 1.2 cm
276 wide, with 9 cm between them. The droplets were impacted by inertia on aluminium plates located 45 mm behind
277 the air inlets. The inlet width and distance between the inlet and impactation plate were selected to be identical to
278 those of the CWS. The air and smaller noncollected droplets were directed to a shared corridor before the air fan.
279 The collected water flowed to the collection funnel under gravity, and the collection bottle was sterilised.

280 The fan can be modulated at 10 intensities (10–100% of the maximum fan speed). The air inlet velocities were
281 measured in front of each of the three slots of the BOOGIE collector at different heights (high, middle, and low
282 points), with the velocity modulated according to these 10 values (**Figure S6**). The measured velocities varied
283 from 2 to approximately 15 m s⁻¹, with an increase of approximately 1.5 m s⁻¹ per intensity step. The air inlet
284 velocity stabilised at 90% of the fan speed (corresponding to a value of 14 m s⁻¹). The velocities measured at
285 different fan intensities were highly homogeneous between slots and for the same slot at different heights, with
286 only a few percentages of standard deviations (between 1.5 to 5%), possibly indicating that the geometry of the
287 collector provided good airflow stabilisation. The next section, in which the flow inside the collector is simulated,
288 provides a more robust assessment of this statement.

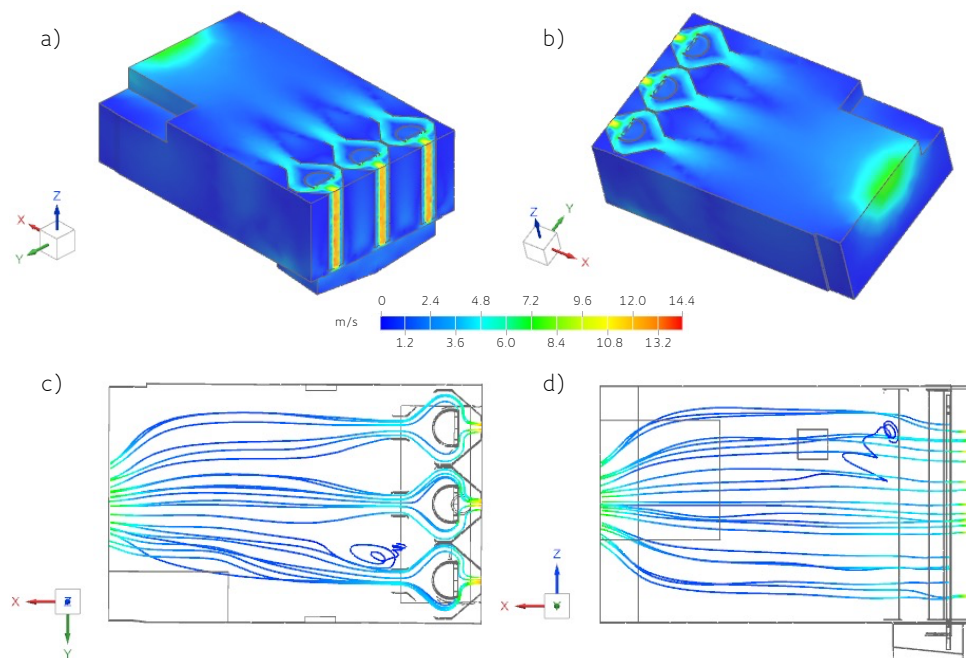
289 3.2 Performance evaluation

290 3.2.1 CFD simulations

291 *Flow velocity*



292 **Figure 2a and b** displays the flow velocity field inside the collector for air outlet flow velocity equal to 8 m s^{-1}
293 (the same for 2 m s^{-1} in **Figure S7a and b**). As noted in Section 2.2.2, the air outlet flow velocity equal to 8 m s^{-1}
294 corresponds to an air inlet flow velocity equal to 12.8 m s^{-1} (1.6 factor), a value similar to the measured air inlet
295 velocity of the collector. We present the horizontal cutting planes at the centre of the fan. Regardless of the air
296 outlet velocity, the colour display of the flow velocity contour is identical.

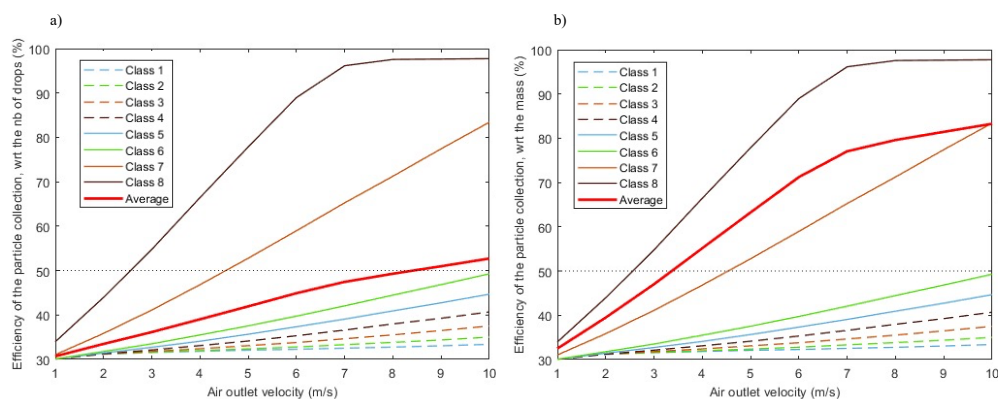


297
298 **Figure 2. a) and b) Cutting plane in the flow velocity contour (in magnitude) in the case of an 8 m s^{-1} air outlet flow**
299 **velocity; c) and d) set of streamlines in the collector (c- right view, d - top view) in the case of an 8 m s^{-1} air outlet flow**
300 **velocity. Colour code indicates the different air velocity inside the collector.**

301 Streamlines were also displayed (**Figures 2c and d** and **S7c and d**), with a set of seed points selected randomly
302 on the air inlet faces. They displayed velocity results by showing the path taken by a massless particle. Each point
303 along a streamline is always tangential to the velocity vector of the fluid flow. Again, the streamlines were only
304 slightly modified between the two velocities.

305 *Particle impact tracking*

306 Various classes of particles were injected into the collector at different air outlet velocities. **Table S2** lists the
307 number of water droplets for each air outlet velocity and each class of particles recorded by the solver in front of
308 the three inlets, represented by the three slots. Arbitrarily, approximately 60 000 particles are injected. We
309 calculated the number of injected droplets that impacted the vertical plates among the 60 000 particles; this allowed
310 the estimation of each class of particle and each velocity of the normalised efficiency of particle collection, as
311 reported in **Figure 3** in terms of the number of droplets and the mass of the droplets.



312

313 **Figure 3. Normalized efficiency of the particle collection, regarding the number of droplets (a) and regarding the mass**
314 **of the droplets (b).**

315 We can observe that as the air outlet velocity increases, so does the collection efficiency for all droplet classes.
316 For classes 7 and 8 (more than 15 μm in term of diameter), the collection efficiencies were $>50\%$ at low air outlet
317 velocities ($<5 \text{ m s}^{-1}$). At higher speeds, collection efficiencies $>80\%$ were achieved for both size classes. At the
318 maximum speed, a collection efficiency of approximately 50% was reached for class 6 (10 μm in diameter). On
319 average, for all droplet sizes, the average collection efficiencies of $>50\%$ in terms of numbers were achieved at air
320 velocities $>8 \text{ m s}^{-1}$. Considering the mass of the droplets, the two largest classes (7 and 8) naturally represented
321 the largest mass of water collected. Because these two classes were efficiently collected even at low air velocities,
322 a collection efficiency of 50% in terms of mass was achieved at 3 m s^{-1} of velocity. At the maximum velocity, the
323 average collection efficiency was approximately 80% in terms of mass.

324 The results highlight that the collector should be used with the highest velocity because the collection efficiency
325 is theoretically maximal. However, at 7 m s^{-1} , we observed a slowdown in the overall collection efficiency because
326 the largest drops were already 100% collected. These results allowed us to estimate the theoretical cutoff diameter,
327 which represented the diameter at which 50% of the drops were collected. In our case, for the simulation
328 conditions, this can be estimated at approximately 10 μm when the air outlet velocity is maximal.

329 These results are subject to limitations and uncertainties related to the modelled physical phenomena. First, the
330 statistical results from the CFD simulations were based on a certain number of particles injected into the
331 computational domain to achieve reasonable computing times. Second, the collection surfaces are supposed to be
332 “ideal”: a droplet, that impacts a plate, sticks to it; therefore, its transport by gravity to the funnel remains
333 hypothetical. Finally, none of the physical phenomena were considered; the simulations were based on the
334 equations of classical fluid mechanics, but other phenomena, such as electrostatics or Brownian motion, may affect
335 the lightest particles. However, the performed simulations indicate good theoretical efficiency of the new BOOGIE
336 collector for collecting cloud droplets, which also confirms that the distance between the air inlet slots and the
337 outlet fan is adequate because it is beneficial for air flow stabilisation.

338 3.2.2 Field sampling experiments



339 To evaluate the performance of the BOOGIE sampler, 17 cloud events were collected at PUY station from May
340 to July 2016 and from July to November 2021. Seventeen cloud events, corresponding to twenty samples, were
341 collected using BOOGIE to evaluate its performance by measuring the collected water mass as a function of the
342 sampled volume of air (Wieprecht et al., 2005; Demoz et al., 1996). **Table S3** reports various parameters measured
343 during the sampling duration: meteorological parameters (temperature and wind speed) and microphysical cloud
344 properties (Liquid Water Content LWC_{meas} , and effective radius, R_{eff} , quantified by a PVM-100 probe et recorded
345 every 5 min).

346 First, we can estimate the cloud water collection rates of BOOGIE equal to $106 \pm 52 \text{ mL h}^{-1}$. Water volume is
347 crucial because it determines the biological and chemical analyses that can be performed in the laboratory. The
348 BOOGIE collection rate allows sufficient cloud water to be obtained in a short duration, which is crucial because
349 the origin of the air mass that reaches the collection site can vary in a short time.

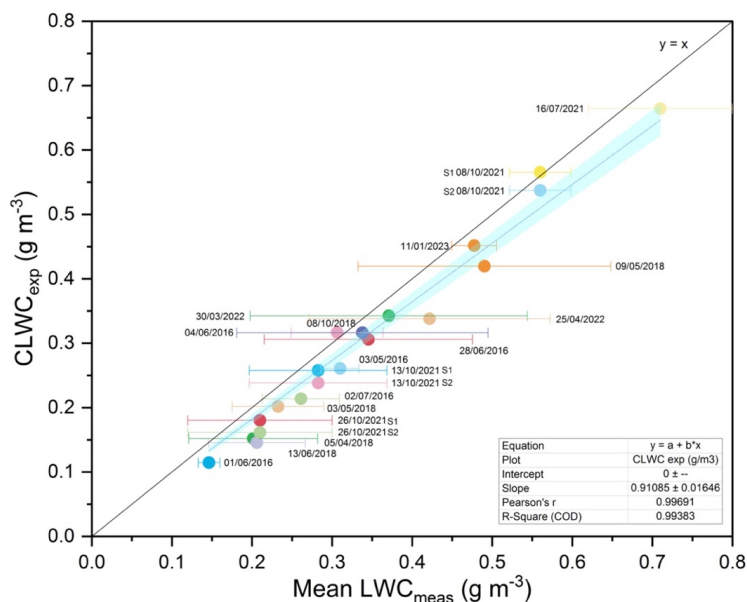
350 Experimentally, we can also evaluate the Collected LWC ($CLWC_{exp}$) in g m^{-3} (Waldman et al., 1985) as:

$$351 \quad CLWC_{exp} = \frac{M}{F \times \Delta t} \quad (1)$$

352 where M is the collected water mass (g); F is the sampler airflow ($\text{m}^3 \text{ min}^{-1}$); and Δt is the sampling duration (min).

353 To evaluate $CLWC_{exp}$, we estimated the sampler airflow of the new cloud collector. The optimal simulated
354 collection efficiency for this collector was simulated for an outlet air velocity equal to 8 m s^{-1} corresponding to a
355 theoretical inlet air velocity of 12.8 m s^{-1} (Section 3.2.1). For cloud-water sampling, the sampler was operated at its
356 maximum inlet air velocity. Using a thermal anemometer directly in front of the slots, we measured an air velocity
357 of 14 m s^{-1} (Section 3.1); therefore, we can estimate the outlet velocity at 8.75 m s^{-1} . To calculate the volume of
358 the sampled air, we use this value for the outlet air velocity; thus, the sampled air flow can be evaluated as follows:
359 with three inlets of 302 mm length and 12 mm width giving a total inlet surface of $10.9 \times 10^{-3} \text{ m}^2$ and an air velocity
360 of 8.75 m s^{-1} , then the airflow is $343.3 \text{ m}^3 \text{ h}^{-1}$ ($5.72 \text{ m}^3 \text{ min}^{-1}$).

361 $CLWC_{exp}$ can be compared with the measured mean LWC_{meas} for the 17 cloud events, as shown in **Figure 4**.



362
 363 **Figure 4.** Collected cloud water content $CLWC_{exp}$ vs measured LWC_{mes} (in $g\ m^{-3}$) for a selection of 17 cloud events
 364 samples at the PUY station. Sampling dates and the standard deviation of the measured LWC are indicated. The black
 365 solid line represents the $y = x$ function; linear fit of the experimental data with an intercept at 0 is represented by the
 366 dotted blue line and the blue area denotes the 95% confidence interval of this fit. S1/S2 corresponds to the same cloud
 367 event sampled with two BOOGIE collectors installed in parallel.

368 The $CLWC_{exp}$ and measured LWC_{mes} were well correlated ($r^2 = 0.99$; the slope of the linear regression was 0.91,
 369 and the intercept was $0\ g\ m^{-3}$). Systematic and random deviations from the “theoretical” efficiency are represented
 370 by a 1:1 line. Among the 17 cloud samples, only 2 cloud events presented a $CLWC_{exp}$ slightly higher than the
 371 LWC_{mes} .

372 The sampling efficiency can be estimated as follows:

373
$$\text{Sampling efficiency (\%)} = \frac{CLWC_{exp}}{LWC_{mes}} \times 100 \quad (2)$$

374
 375 The average calculated sampling efficiency over 17 cloud events was equal to $87.2 \pm 8.6\%$. The sampling
 376 efficiency appeared to decrease when there was a shift to higher LWC_{mes} , which has also been observed with
 377 other samplers such as the CASCC2, possibly explained by interior collector wall losses for large droplets
 378 (Wieprecht et al., 2005). A plausible explanation for our sampler is the coalescence of very large droplets on the
 379 front face before aspiration into the slits.

380 The mean cloud wind speed and effective cloud droplet radius varied between the cloud events. **Figure S8** shows
 381 the sampling efficiency vs the three meteorological and microphysical parameters. The 17 clouds were sampled
 382 under conditions typically encountered at PUY for cloud sampling under warm conditions and for different
 383 seasons: temperatures $>0\ ^\circ C$ with a maximum value of approximately $11\ ^\circ C$; wind speed varying from 0.2 to 13
 384 $m\ s^{-1}$. No tendency was observed between the sampling efficiency and temperature, supporting the fact that the
 385 collector can be operated over different seasons. The collector's orientation towards the wind is important,
 386 particularly under strong wind conditions. Incorrect orientation (*i.e.*, not in front of the wind) could drastically



387 reduce collection efficiency, whereas orientation towards strong winds could improve collection efficiency. For
388 the collected cloud events, we observed that the collection efficiency slightly decreased with wind speed; however,
389 the strength of the association was small (Pearson correlation coefficient of -0.23). At high wind speeds (gusts)
390 near 10 m s^{-1} , cloud droplet sampling can be non-isokinetic, explaining the possible perturbation of collection
391 efficiency. The average effective radius varied from 4.6 to $11 \mu\text{m}$; there was no correlation between this parameter
392 and the collection efficiency, indicating adequate collection performance of the collector even for smaller droplets.

393 The collection efficiency calculated herein uses the theoretical total cloud water based on integrated measurement
394 methods (LWC). These estimates must be treated with caution because they are marred by several
395 errors/approximations listed here. These can be the result of the limitations of the instruments themselves (the
396 collector and the PVM probe) and the sampling conditions (wind); with the PWM-100 probe, we cannot optimally
397 capture the time evolution of the LWC because data are recorded every 5 min. Finally, the theoretical sampler
398 airflow used to calculate CLWC_{exp} is intrinsically an estimate, and this can be additionally perturbed by the wind
399 condition. Nevertheless, this first comparison provides a rough estimate of the collection performance of the
400 BOOGIE collector, which appears to be suitable for contrasting environmental conditions.

401 3.3 Comparison of cloud samplers

402 A field campaign was conducted at PUY in 2016 to compare the new collector with other commonly used samplers.
403 The BOOGIE collector has been deployed to sample clouds together with the CWS used at the PUY station since
404 2001 and the CASCC2 (Figure S9). From 1st June to 2nd July, four cloud events were simultaneously collected
405 using these three samplers. The meteorological conditions and microphysical cloud properties were monitored
406 during the cloud events (Figure S10). Back trajectories were computed using the CAT model for the four cloud
407 events (Figure S11). The three samplers were oriented in front of the wind at the beginning of the sampling period;
408 changes in the wind direction were checked during this period, and the orientation of the collectors was modified
409 accordingly.

410 The prevailing winds during the first two cloud events (01 and 04/06/2016) arrived from the north-northwest and
411 north-northeast directions, whereas the other two (28/06/2016 and 02/07/2016) were locally associated with winds
412 coming from the southwest direction. This last event was also characterised by strong wind speeds of up to 14 m s^{-1}
413 at the end of the sampling time. For the four cloud events, the wind directions did not drastically change during
414 the sampling duration except for on the 4th June where some fluctuations were observed; however, these were not
415 significant because the wind speed was extremely low (0.2 m s^{-1}). Regarding the microphysical properties, the first
416 cloud event presented lower mean measured LWC (0.15 g m^{-3}) in comparison to the others (approximately 0.3 g m^{-3})
417 m^{-3}). In contrast, the average radius was highest for the first cloud event (approximately 22 vs $9\text{--}13 \mu\text{m}$ in
418 diameter). The temperature corresponded to warm cloud conditions (between 6 and $10 \text{ }^\circ\text{C}$), allowing the collection
419 of liquid droplets.

420 *Sampling efficiency*

421 First, the cloud water samplers were compared in terms of sampling efficiency, considering the calculated
422 CLWC_{exp} and measured LWC_{mes} (equation (2)). For the CASCC2, the sampled airflow was evaluated following
423 Demoz et al. (1996) (Section 2.3.2). The sampled airflow was evaluated for the CWS, which is a homemade
424 collector that follows the recommendations of Kruisiz et al. (1993). As indicated in Section 2.3.2, the air inlet flow



425 velocity was measured as 13.5 m s^{-1} . Because the CWS and BOOGIE collectors have the same geometry as the
 426 impaction system, we applied the ratio (1.6) evaluated for the BOOGIE collector to calculate the outlet velocity
 427 (8.43 m s^{-1}). Therefore, considering the surface of the entry slot, the sampled air entering the CWS collector was
 428 estimated to be equal to $113.9 \text{ m}^3 \text{ h}^{-1}$ ($1.90 \text{ m}^3 \text{ min}^{-1}$).

429 **Table 1. Information on cloud water collection performed with BOOGIE, CWS and CASCC2 samplers for four**
 430 **independent cloud events at PUY. The temperature, wind speed and R_{eff} are averaged over the sampling time.**

Cloud events: duration, mean temperature, mean wind speed & mean effective radius	Sampler	BOOGIE	CWS	CASCC2
		Sampled airflow ($\text{m}^3 \text{ h}^{-1} / \text{m}^3 \text{ min}^{-1}$)	343.3/5.72	113.9/1.90
Date = 01/06/2016	LWC _{mes} (g m^{-3})		0.15 ± 0.01	
Duration = 90 min	Sampled volume of air	514.8	170.8	425.7
T = $6.3 \pm 0.2 \text{ }^\circ\text{C}$	Collected water (g)	59	19	40
Wind speed = $8.1 \pm 0.5 \text{ m s}^{-1}$	CLWC _{exp} (g m^{-3})*	0.115	0.12	0.094
$R_{\text{eff}} = 10.8 \pm 0.7 \text{ }\mu\text{m}$	Sampling efficiency (%)*	79	76	64
Date = 04/06/2016	LWC _{mes} (g m^{-3})		0.31 ± 0.06	
Duration = 180 min	Sampled volume of air	1029.6	341.6	851.4
T = $7.8 \pm 0.2 \text{ }^\circ\text{C}$	Collected water (g)	326	110	261
Wind speed = $0.3 \pm 0.1 \text{ m s}^{-1}$	CLWC _{exp} (g m^{-3})*	0.317	0.322	0.307
$R_{\text{eff}} = 6.6 \pm 0.6 \text{ }\mu\text{m}$	Sampling efficiency (%)*	103	105	101
Date = 28/06/2016	LWC _{mes} (g m^{-3})		0.35 ± 0.13	
Duration = 60 min	Sampled volume of air	343.2	113.9	283.8
T = $9.3 \pm 0.14 \text{ }^\circ\text{C}$	Collected water (g)	105	34	88
Wind speed = $2.3 \pm 0.4 \text{ m s}^{-1}$	CLWC _{exp} (g m^{-3})*	0.306	0.30	0.310
$R_{\text{eff}} = 4.6 \pm 1.0 \text{ }\mu\text{m}$	Sampling efficiency (%)*	89	87	89
Date = 02/07/2016	LWC _{mes} (g m^{-3})		0.26 ± 0.05	
Duration = 360 min	Sampled volume of air	2059.2	683.3	1702.8
T = $9.7 \pm 1 \text{ }^\circ\text{C}$	Collected water (g)	440	135	290
Wind speed = $12.0 \pm 1.5 \text{ m s}^{-1}$	CLWC _{exp} (g m^{-3})*	0.213	0.198	0.170
$R_{\text{eff}} = 6.1 \pm 0.7 \text{ }\mu\text{m}$	Sampling efficiency (%)*	82	76	65

* The collected LWC (CLWC_{exp}) is calculated following equation (1) and the sampling efficiency by equation (2).

431
 432 The CASCC2 and BOOGIE samplers collected approximately 300 m^3 of air per hour, whereas the sampled volume
 433 of air collected by the CWS was markedly lower (approximately $100 \text{ m}^3 \text{ h}^{-1}$), which explains the lower amount of
 434 collected water. The BOOGIE sampler presented a mean water collection rate for the four cloud events of 82 ± 32
 435 mL h^{-1} which was significantly higher than the two that of the other collectors (CASCC2: $62 \pm 30 \text{ mL h}^{-1}$; CWS :
 436 $26 \pm 11 \text{ mL h}^{-1}$) (t-test, $p < 0.05$). On average, the calculated sampling efficiencies were $88 \pm 11\%$, $86 \pm 14\%$, and
 437 $79 \pm 18\%$ for BOOGIE, CWS, and CASCC2, respectively. Overall, the three collectors exhibited similar and
 438 satisfactory collection efficiencies. This confirms that the volume of water collected by cloud samplers can be used
 439 as a proxy to estimate cloud LWC. The slightly lower collection efficiency of CASCC2 may reflect the loss of
 440 droplets off the strands and/or losses inside the collector on the walls, as highlighted by Wieprecht et al. (2005),
 441 particularly for large droplets. This collector appeared to be more affected by the intensity of wind speed, with the
 442 lowest collection efficiencies observed for the two windier cloud events. As reported by Krusiz et al. (1992) for



443 CWS and shown in this study for BOOGIE, no correlation of wind speeds to the $CLWC_{exp}$ of the samplers was
444 found. In the case of the 4th June cloud, the appearance of fine rain during sampling could possibly explain the
445 overestimation of collection efficiency observed for all collectors, as we did not observe conditions such as strong
446 winds that could disrupt the sampling.

447 Concerning the CASCC2, a sampling efficiency was previously determined during the FEBUKO experiments in
448 the Thüringer Wald (Germany) at $56 \pm 17\%$ (Wieprecht et al., 2005). Kruijz et al. (1993) calculated a sampling
449 efficiency of approximately 60% for the CWS during sampling experiments performed at Mount Sonnblick
450 (Austria). This sampling efficiency seems to be lower than that calculated in the present study. This could be
451 influenced by environmental conditions and cloud microphysical properties, which differ between collection sites.
452 The four cloud events have also been sampled at PUY under “optimal” conditions (summertime conditions with
453 limited wind speed and sufficient cloud LWC), possibly explaining the efficient collection of the samplers.

454 *Cloud water chemical and biological composition*

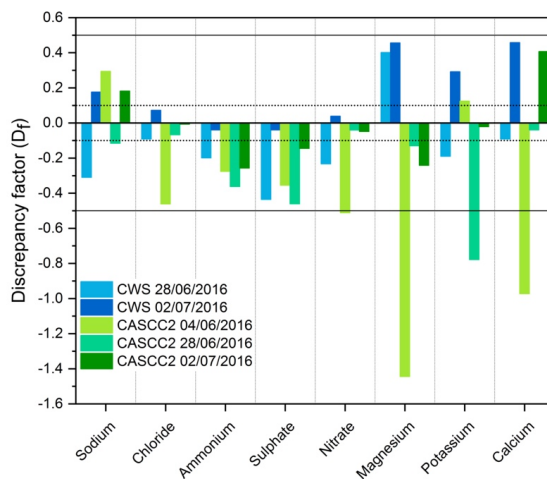
455 To compare the three cloud water collectors, we also focused on the chemical compositions of the three cloud
456 water samples collected in 2016. The concentrations of inorganic ions in samples collected with the CWS and
457 CASCC2 collectors (**Table S4, Figure S12**) were compared to the concentrations measured in samples collected
458 with BOOGIE using the discrepancy factor (D_f) calculated using **equations 3a and 3b**.

$$459 \quad D_{f,CWS} = \frac{C_{BOOGIE} - C_{CWS}}{\left(\frac{C_{BOOGIE} + C_{CWS}}{2}\right)} \quad (3a)$$

$$460 \quad D_{f,CASCC2} = \frac{C_{BOOGIE} - C_{CASCC2}}{\left(\frac{C_{BOOGIE} + C_{CASCC2}}{2}\right)} \quad (3b)$$

461 where C_{BOOGIE} is the concentration of ions measured in samples collected with BOOGIE, and C_{CWS} and C_{CASCC2}
462 are the concentrations of ions measured with CWS and CASCC2, respectively.

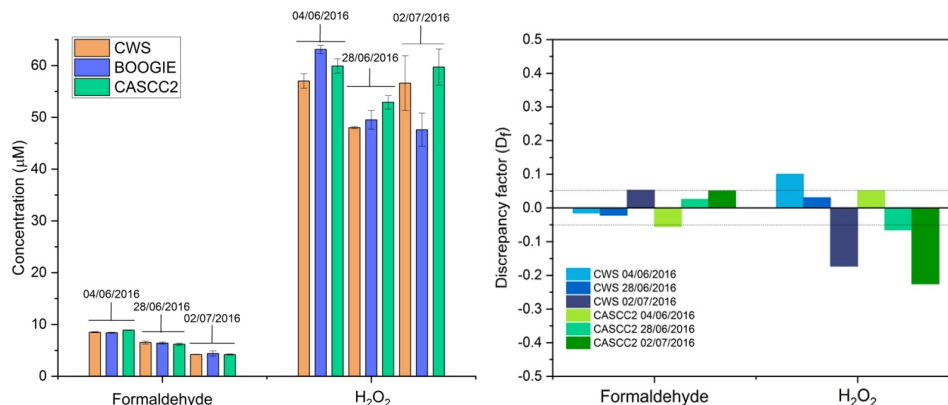
463 **Figure 5** shows the estimated $D_{f,CWS}$ and $D_{f,CASCC2}$ for anions and cations for cloud samples. The horizontal dashed
464 lines represent the analytical error on the measurement, which is comparable with $D_{f,CWS}$ 02/07/2016 for sulphate,
465 nitrate, chloride, and ammonium and $D_{f,CASCC2}$ 28/06/2016 and 02/07/2016 for nitrate, sulphate, chloride, and
466 sodium. The other D_f values were higher, but generally <0.5 , which could represent a good comparability of the
467 cloud collectors, because the chemical composition of cloud condensation nuclei may be inhomogeneous. At first
468 glance, concentrations with the CASCC2 appear to be slightly higher, but not for all ionic species and not for all
469 the cloud events. These three samplers present specific designs and surfaces of collection (plate for BOOGIE and
470 CWS vs strands for CASCC2), leading to different estimated cutoff diameters (10 μm for BOOGIE, 7.5 μm for
471 CWS, and 3.5 μm for CASCC2) and possibly to small differences in the chemical composition of the samples.
472



473

474 **Figure 5. Histograms presenting discrepancy factors (D_f) between BOOGIE and CWS and CASCC2 calculated using**
475 **anion and cation concentrations for the three cloud samples. The dashed lines represent the analytical error, whereas**
476 **the plain line represents the 50% discrepancy.**

477 Formaldehyde and hydrogen peroxide concentrations have been also measured in samples obtained with the three
478 collectors. Concentrations and discrepancy factors between collectors are presented in **Figure 6**. These results are
479 consistent with what was observed with the ionic content because the collectors indicate D_f values mostly within
480 the analytical error and maximum measured D_f values <0.5 .



481 **Figure 6. Left: Histograms presenting the anion and cation concentrations for the three cloud samples collected using**
482 **CWS, BOOGIE, and CASCC2 in parallel. The error bars correspond to the standard deviation. Right: Histograms**
483 **presenting discrepancy factors (D_f) between the BOOGIE and CWS and CASCC2. The dashed lines represent the**
484 **analytical error.**

485 To further evaluate BOOGIE, two identical collectors were installed at the PUY station in 2021 to check for
486 differences in the chemical composition of cloud waters collected in parallel. For clouds on 08/07/2021, chemical
487 measurements were performed in triplicate to analyse the statistical differences (**Figure S13, Table S5**). The error
488 bars depict the analysis error, which is higher than the discrepancy between the BOOGIE collectors for sodium,
489 potassium, calcium, and chloride. The black plain line represents the p-value obtained for the t-test (right y-axis);
490 if the p-value is <0.05 , represented in the plot by the yellow dashed line, the difference between the two BOOGIE



491 collectors is significant, as observed for magnesium, nitrate, and chloride. Nevertheless, the difference was not
492 significant for sodium, ammonium, potassium, calcium, and sulphate, indicating good reproducibility of sampling
493 with the BOOGIE collectors.

494 Given the uncertainties in laboratory measurements and the possible intrinsic variability of the chemical
495 composition within the cloud system, we can reasonably argue that the chemical compositions of the collectors
496 are comparable. Schell et al. (1992) compared two single-stage cloud impactors with different designs and
497 highlighted the large differences between the ionic compositions of the samples. These differences have been
498 discussed to be related to different microphysical properties of the sampled clouds that induced bias in the
499 collection: smaller droplets can be sampled with a lower cutoff diameter of the collector, and a lower LWC can
500 eventually induce some evaporation of the smaller droplets. The three cloud events presented “stable”
501 microphysical properties during their collection period (Figure S9). This could explain the good agreement
502 between the collectors in terms of their chemical composition. Wieprecht et al. (2005) compared the chemical
503 composition of cloud water collected with a low-volume single-stage slit jet impactor and with the CASCC2 string
504 collector and reported 8–15% differences in the solute ionic mass in cloud water, in the range observed in the
505 present study (4–35% of differences, average of 12%) between the three collectors.

506 The microbial energetic state given by the in-cell ATP and ADP concentrations from each cloud sample was
507 assessed during the inter-comparison campaign (see Supplementary Information for a description of the protocol).
508 The ATP/ADP ratio gives the energetic stress of the cloud water microbiota; a ratio <0.6 indicates a good energetic
509 state, 0.6 to 1, a medium one, and >1, a low energetic state. The measured ratios are listed in Table S6. The
510 ATP/ADP ratio ranged from 0.2 to 0.4, revealing a good energetic state of microflora for each sample. The
511 measured ATP/ADP ratios were similar for the cloud water samples from the three collectors. Thus, we argue that
512 the three samplers could be considered non-stressful and suitable for cloud microbiota collection.

513 4 Conclusions

514 This study presented a new cloud collector called BOOGIE. This single-stage collector allows cloudy air
515 containing aqueous droplets to be drawn through three air inlets in the form of vertically oriented slots. The cloud
516 droplets were collected using vertical plates placed behind the slots, allowing them to be impacted. They then
517 flowed by gravity along the plates, fell into a funnel, and ended up in a sterilised glass bottle. It was made of
518 aluminium, but can be manufactured from other materials, such as plastic materials such as nylon or PTFE to
519 investigate transition metal ions in cloud waters. The cloud collector can be connected to the mains or run on
520 batteries (12 V voltage); thus, the collector can be operated at its own power during field measurement campaigns
521 for at least 4 h using a 2 kg small battery. Parts of the sampler were removed for cleaning; the front face, impaction
522 chamber, funnel, and glass bottle were sterilised in an autoclave. This allowed for the characterisation of the
523 biological content of the sampled clouds (biodiversity, concentration, and viability/activity) (Vařtilingom et al.,
524 2012). Biological and chemical collector blanks were easily prepared by spraying MilliQ water onto the collection
525 plates and collecting the water flowing into the collection glass bottle.

526 CFD simulations were performed to investigate how the collector captured cloud droplets. First, considering the
527 3D-dimensional structure of the collector, some turbulences were simulated inside the collector, which was
528 reassuring. Different classes of cloud droplets were injected into the collector to simulate their impacts on the



529 collection plates. This theoretical study indicates that on average, for all droplet sizes (radius from 2.5 to 10 μm),
530 the average collection efficiencies of $>50\%$ in terms of numbers were achieved at air outlet velocities $>8 \text{ m s}^{-1}$. A
531 collection efficiency of approximately 50% was reached for 5 μm droplets in a radius that gave us an estimate of
532 the 50% cutoff diameter of the collector (approximately 10 μm). This estimate seems slightly higher than the cutoff
533 diameters of other cloud samplers (more in the range between 3.5 and 10 μm in diameter). However, comparisons
534 of cutoff diameters between samplers are difficult because these estimates are made using different methods; in
535 particular, the theoretical collection efficiency often considers the Stokes number (Demoz et al., 1996).

536 Based on the 17 cloud events sampled at the PUY station, a mean water collection efficiency was calculated as
537 $156 \pm 52 \text{ mL h}^{-1}$ for clouds presenting various microphysical cloud properties: the mean LWC was between 0.15
538 and 0.71 g m^{-3} and the mean effective radius R_{eff} was between 4.6 and 11 μm . This made it possible to obtain
539 sufficient water volumes over short periods for targeted chemical and biological analyses. This is crucial for
540 minimally integrating the cloud properties in space and time. Methodological developments in recent years have
541 made it possible to assess the organic composition and biodiversity of this aqueous environment using non-targeted
542 methods (Rossi et al., 2023; Bianco et al., 2018). This requires large volumes of cloud water (hundreds of milliliters
543 or even liters of water), which can be collected rapidly using the new collector alone or by duplicating it.

544 Considering the measured LWC, LWC_{meas} , the sampling efficiency of this new collector was estimated at $87.2 \pm$
545 8.6% over the same set of cloud events collected at PUY. No significant decrease in the collection efficiency was
546 observed as the wind speed increased, over the range of variation between 0.3 and 13 m s^{-1} . No significant
547 correlation was observed between the efficiency and mean measured effective radius. A low LWC cloud event
548 would present a greater proportion of liquid water residing in smaller droplets; therefore, for a low LWC, we
549 expected the collection efficiency to diminish owing to the cutoff diameter. However, this decrease was not
550 observed in the cloud samples. Additional measurements of droplet size distribution during sampling would be
551 beneficial for clarifying this issue.

552 This new cloud water collector was compared with two other single-stage collectors that are commonly used by
553 the scientific community to study cloud composition and environmental variability. We selected the CWS initially
554 developed at the University of Vienna (Kruiz et al., 1993) and often deployed at mountainous sites such as Mount
555 Sonnblick (Austria) and the PUY station. The impaction of the droplets occurs in a metallic plate horizontally
556 installed in the collector, and it can be sampled under supercooled conditions. The other collector was one of the
557 samplers developed by the California Institute of Technology (Caltech) for studies on fog and clouds (Daube et
558 al., 1987), the CASCC2. This active sampler is a compact version of the CASCC, in which droplets are collected
559 by impaction on a set of six rows of stainless-steel strings; it is highly efficient in terms of collection and is not
560 affected by raindrops owing to its design. It cannot function under supercooled conditions. The proposed BOOGIE
561 collector aims to efficiently sample cloud droplets under warm cloud conditions and is designed to be easily
562 sterilisable. Under low wind conditions, it is not affected by rain.

563 We compared the collection efficiency and chemical compositions of these three collectors. For the four studied
564 cloud events, the BOOGIE collector presented an elevated water collection rate of $82 \pm 32 \text{ mL h}^{-1}$ (CASCC2: 62
565 $\pm 30 \text{ mL h}^{-1}$; CWS: $26 \pm 11 \text{ mL h}^{-1}$). This can be explained by the increased volume of cloudy air entering the new
566 collector. On average, the calculated sampling efficiency was $88 \pm 11\%$ for BOOGIE, in the same range as that
567 for CWS and CASCC2. The chemical and biological compositions measured in the samples collected by the three



568 collectors can be evaluated as comparable; however, some differences can be highlighted, which can be explained
569 by the design of the collector, type of collection, and inhomogeneous chemical composition of the cloud
570 condensation nuclei.

571 This new BOOGIE collector is designed for use in field campaigns and long-term observatory sites. It contributes
572 to the evaluation of the complex cloud water bio-physico-chemical composition, to the analysis of its
573 environmental variability; it allows a sufficient volume of water to be collected to characterize the chemical and
574 biological transformations occurring in it. This will help better constrain detailed cloud chemistry models that need
575 to be validated (Barth et al., 2021). For future development, our team aims to reduce the size and weight of the
576 collector such that it can be installed under a native balloon. The second development concerns the automation of
577 this collector to initiate collection remotely and increase the sampling frequency. Finally, we aim to conduct
578 intensive campaigns in the frame of the ACTRIS “Cloud In Situ” network to compare the collectors used by the
579 scientific community at other measurement sites.

580 *Data availability:* All data are available through communication with the authors.

581 *Author contributions:* LD, MV were responsible of the project. MV, CBern and LD designed the new instrument,
582 MR created the 3D plans of BOOGIE. CBert performed the CFD analysis. MV, AB and LD conducted the cloud
583 sampling. MV and AB performed the chemical and biological analysis in the lab. LD and MV performed the data
584 analysis. LD, MV and AB conducted scientific analyses. LD prepared the manuscript and designed the figures,
585 with contributions from all authors. MV, AB, MR, CBert revised the manuscript.

586 *Competing interests.* The authors declare that they have no conflict of interest.

587 *Acknowledgments.* This study on cloud water characterisation was performed in the framework of the CO-PDD
588 instrumented site of the OPGC observatory and LAMP laboratory. This study was supported by the Université
589 Clermont Auvergne, Centre National de la Recherche Scientifique (CNRS), and Centre National d’Etudes
590 Spatiales (CNES). The authors are also grateful for the support from the Fédération des Recherches en
591 Environnement through the CPER funded by Region Auvergne–Rhône-Alpes, the French Ministry, ACTRIS
592 Research Infrastructure, and FEDER European regional funds. The authors also thank I-Site CAP 20-25. We thank
593 Olivier Masson from the IRSN for their CASCC2 collector, which was gratefully lent during the inter-comparison
594 campaign.

595 *Financial support.* The authors are grateful to the Agence Nationale de la Recherche (ANR) for its financial
596 support through the BIOCAP (ANR-13-BS06-0004) and METACLOUD (ANR-19-CE01-0004) projects. The first
597 project has financed the work of Mickaël Vaïtilingom during his post-doc at the LAMP laboratory and the second
598 one allowed for their evaluation for specific scientific questions. We thank OPGC for additional funding and
599 OPGC Service de developpement technologique for manufacturing the cloud samplers. The Institut de Chimie de



600 Clermont-Ferrand and Laboratoire Microorganismes: Génome Environnement laboratories are acknowledged for
601 allowing access to their chemical and microbial analytical platforms.

602 References

- 603 Adachi, K., Tobo, Y., Koike, M., Freitas, G., Zieger, P., and Krejci, R.: Composition and mixing state of Arctic
604 aerosol and cloud residual particles from long-term single-particle observations at Zeppelin Observatory, Svalbard,
605 *Atmos. Chem. Phys.*, 22, 14421-14439, 10.5194/acp-22-14421-2022, 2022.
- 606 Amato, P., Ménager, M., Sancelme, M., Laj, P., Mailhot, G., and Delort, A.-M.: Microbial population in cloud
607 water at the puy de Dôme: Implications for the chemistry of clouds, *Atmos. Environ.*, 39, 4143-4153,
608 <https://doi.org/10.1016/j.atmosenv.2005.04.002>, 2005.
- 609 Amato, P., Joly, M., Besaury, L., Oudart, A., Taib, N., Moné, A. I., Deguillaume, L., Delort, A.-M., and Debroas,
610 D.: Active microorganisms thrive among extremely diverse communities in cloud water, *PLOS ONE*, 12,
611 e0182869, 10.1371/journal.pone.0182869, 2017.
- 612 Baray, J. L., Deguillaume, L., Colomb, A., Sellegri, K., Freney, E., Rose, C., Van Baelen, J., Pichon, J. M., Picard,
613 D., Fréville, P., Bouvier, L., Ribeiro, M., Amato, P., Banson, S., Bianco, A., Borbon, A., Bourcier, L., Bras, Y.,
614 Brigante, M., Cacault, P., Chauvigné, A., Charbouillot, T., Chaumerliac, N., Delort, A. M., Delmotte, M., Dupuy,
615 R., Farah, A., Febvre, G., Flossmann, A., Gourbeyre, C., Hervier, C., Hervo, M., Huret, N., Joly, M., Kazan, V.,
616 Lopez, M., Mailhot, G., Marinoni, A., Masson, O., Montoux, N., Parazols, M., Peyrin, F., Pointin, Y., Ramonet,
617 M., Rocco, M., Sancelme, M., Sauvage, S., Schmidt, M., Tison, E., Vaïtilingom, M., Villani, P., Wang, M., Yver-
618 Kwok, C., and Laj, P.: Cézeaux-Aulnat-Opme-Puy De Dôme: a multi-site for the long-term survey of the
619 tropospheric composition and climate change, *Atmos. Meas. Tech.*, 13, 3413-3445, 10.5194/amt-13-3413-2020,
620 2020.
- 621 Barth, M. C., Ervens, B., Herrmann, H., Tilgner, A., McNeill, V. F., Tsui, W. G., Deguillaume, L., Chaumerliac,
622 N., Carlton, A., and Lance, S. M.: Box model intercomparison of cloud chemistry, *J. Geophys. Res.: Atmos.*, 126,
623 e2021JD035486, <https://doi.org/10.1029/2021JD035486>, 2021.
- 624 Bauer, H., Kasper-Giebl, A., Löflund, M., Giebl, H., Hitzemberger, R., Zibuschka, F., and Puxbaum, H.: The
625 contribution of bacteria and fungal spores to the organic carbon content of cloud water, precipitation and aerosols,
626 *Atmos. Res.*, 64, 109-119, [https://doi.org/10.1016/S0169-8095\(02\)00084-4](https://doi.org/10.1016/S0169-8095(02)00084-4), 2002.
- 627 Berner, A.: The collection of fog droplets by a jet impaction stage, *STOTEN*, 73, 217-228,
628 [https://doi.org/10.1016/0048-9697\(88\)90430-5](https://doi.org/10.1016/0048-9697(88)90430-5), 1988.
- 629 Bianco, A., Deguillaume, L., Chaumerliac, N., Vaïtilingom, M., Wang, M., Delort, A.-M., and Bridoux, M. C.:
630 Effect of endogenous microbiota on the molecular composition of cloud water: a study by Fourier-transform ion
631 cyclotron resonance mass spectrometry (FT-ICR MS), *Sci. Rep.*, 9, 7663, 10.1038/s41598-019-44149-8, 2019.
- 632 Bianco, A., Deguillaume, L., Vaïtilingom, M., Nicol, E., Baray, J.-L., Chaumerliac, N., and Bridoux, M.:
633 Molecular characterization of cloud water samples collected at the puy de Dôme (France) by Fourier Transform
634 Ion Cyclotron Resonance Mass Spectrometry, *Environ. Sci. & Technol.*, 52, 10275-10285,
635 10.1021/acs.est.8b01964, 2018.
- 636 Bianco, A., Vaïtilingom, M., Bridoux, M., Chaumerliac, N., Pichon, J.-M., Piro, J.-L., and Deguillaume, L.: Trace
637 metals in cloud water sampled at the Puy de Dôme station, *Atmosphere*, 8, 225,
638 <https://doi.org/10.3390/atmos8110225>, 2017.



- 639 Blando, J. D. and Turpin, B. J.: Secondary organic aerosol formation in cloud and fog droplets: a literature
640 evaluation of plausibility, *Atmos. Environ.*, 34, 1623-1632, 10.1016/s1352-2310(99)00392-1, 2000.
- 641 Brantner, B., Fierlinger, H., Puxbaum, H., and Berner, A.: Cloudwater chemistry in the subcooled droplet regime
642 at Mount Sonnblick (3106 M A.S.L., Salzburg, Austria), *Water, Air, and Soil Poll.*, 74, 363-384,
643 10.1007/BF00479800, 1994.
- 644 Collett Jr, J. L., Daube Jr, B. C., Gunz, D., and Hoffmann, M. R.: Intensive studies of Sierra Nevada cloudwater
645 chemistry and its relationship to precursor aerosol and gas concentrations, *Atmos. Environ.*, 24, 1741-1757,
646 10.1016/0960-1686(90)90507-j, 1990.
- 647 Cook, R. D., Lin, Y. H., Peng, Z., Boone, E., Chu, R. K., Dukett, J. E., Gunsch, M. J., Zhang, W., Tolic, N., Laskin,
648 A., and Pratt, K. A.: Biogenic, urban, and wildfire influences on the molecular composition of dissolved organic
649 compounds in cloud water, *Atmos. Chem. Phys.*, 17, 15167-15180, 10.5194/acp-17-15167-2017, 2017.
- 650 Crosbie, E., Brown, M. D., Shook, M., Ziemba, L., Moore, R. H., Shingler, T., Winstead, E., Thornhill, K. L.,
651 Robinson, C., MacDonald, A. B., Dadashazar, H., Sorooshian, A., Beyersdorf, A., Eugene, A., Collett Jr, J., Straub,
652 D., and Anderson, B.: Development and characterization of a high-efficiency, aircraft-based axial cyclone cloud
653 water collector, *Atmos. Meas. Tech.*, 11, 5025-5048, 10.5194/amt-11-5025-2018, 2018.
- 654 Daube, B., Kimball, K. D., Lamar, P. A., and Weathers, K. C.: Two new ground-level cloud water sampler designs
655 which reduce rain contamination, *Atmos. Environ.*, 21, 893-900, [https://doi.org/10.1016/0004-6981\(87\)90085-0](https://doi.org/10.1016/0004-6981(87)90085-0),
656 1987.
- 657 Deguillaume, L., Leriche, M., Amato, P., Ariya, P. A., Delort, A. M., Pöschl, U., Chaumerliac, N., Bauer, H.,
658 Flossmann, A. I., and Morris, C. E.: Microbiology and atmospheric processes: chemical interactions of primary
659 biological aerosols, *Biogeosciences*, 5, 1073-1084, 10.5194/bg-5-1073-2008, 2008.
- 660 Deguillaume, L., Charbouillot, T., Joly, M., Vaïtilingom, M., Parazols, M., Marinoni, A., Amato, P., Delort, A.
661 M., Vinatier, V., Flossmann, A., Chaumerliac, N., Pichon, J. M., Houdier, S., Laj, P., Sellegri, K., Colomb, A.,
662 Brigante, M., and Mailhot, G.: Classification of clouds sampled at the puy de Dôme (France) based on 10 yr of
663 monitoring of their physicochemical properties, *Atmos. Chem. Phys.*, 14, 1485-1506, 10.5194/acp-14-1485-2014,
664 2014.
- 665 Demoz, B. B., Collett, J. L., and Daube, B. C.: On the Caltech active strand cloudwater collectors, *Atmos. Res.*,
666 41, 47-62, [https://doi.org/10.1016/0169-8095\(95\)00044-5](https://doi.org/10.1016/0169-8095(95)00044-5), 1996.
- 667 Dominutti, P. A., Renard, P., Vaïtilingom, M., Bianco, A., Baray, J. L., Borbon, A., Bourianne, T., Burnet, F.,
668 Colomb, A., Delort, A. M., Dufлот, V., Houdier, S., Jaffrezo, J. L., Joly, M., Lereboure, M., Metzger, J. M.,
669 Pichon, J. M., Ribeiro, M., Rocco, M., Tulet, P., Vella, A., Leriche, M., and Deguillaume, L.: Insights into tropical
670 cloud chemistry in Réunion (Indian Ocean): results from the BIO-MAÏDO campaign, *Atmos. Chem. Phys.*, 22,
671 505-533, 10.5194/acp-22-505-2022, 2022.
- 672 Ehrenhauser, F. S., Khadapkar, K., Wang, Y., Hutchings, J. W., Delhomme, O., Kommalapati, R. R., Herckes, P.,
673 Wornat, M. J., and Valsaraj, K. T.: Processing of atmospheric polycyclic aromatic hydrocarbons by fog in an urban
674 environment, *Journal of Environmental Monitoring*, 14, 2566-2579, 10.1039/C2EM30336A, 2012.
- 675 Gioda, A., Mayol-Bracero, O. L., Scatena, F. N., Weathers, K. C., Mateus, V. L., and McDowell, W. H.: Chemical
676 constituents in clouds and rainwater in the Puerto Rican rainforest: Potential sources and seasonal drivers, *Atmos.*
677 *Environ.*, 68, 208-220, <https://doi.org/10.1016/j.atmosenv.2012.11.017>, 2013.



- 678 Gioda, A., Reyes-Rodríguez, G. J., Santos-Figueroa, G., Collett Jr., J. L., Decesari, S., Ramos, M. d. C. K. V.,
679 Bezerra Netto, H. J. C., de Aquino Neto, F. R., and Mayol-Bracero, O. L.: Speciation of water-soluble inorganic,
680 organic, and total nitrogen in a background marine environment: Cloud water, rainwater, and aerosol particles,
681 *Journal of Geophys. Res.: Atmos.*, 116, <https://doi.org/10.1029/2010JD015010>, 2011.
- 682 Guo, J., Wang, Y., Shen, X., Wang, Z., Lee, T., Wang, X., Li, P., Sun, M., Collett Jr, J. L., Wang, W., and Wang,
683 T.: Characterization of cloud water chemistry at Mount Tai, China: Seasonal variation, anthropogenic impact, and
684 cloud processing, *Atmos. Environ.*, 60, 467-476, <http://dx.doi.org/10.1016/j.atmosenv.2012.07.016>, 2012.
- 685 Herckes, P., Valsaraj, K. T., and Collett Jr, J. L.: A review of observations of organic matter in fogs and clouds:
686 Origin, processing and fate, *Atmos. Res.*, 132–133, 434-449, [10.1016/j.atmosres.2013.06.005](https://doi.org/10.1016/j.atmosres.2013.06.005), 2013.
- 687 Herckes, P., Hannigan, M. P., Trenary, L., Lee, T., and Collett Jr, J. L.: Organic compounds in radiation fogs in
688 Davis (California), *Atmos. Res.*, 64, 99-108, [10.1016/s0169-8095\(02\)00083-2](https://doi.org/10.1016/s0169-8095(02)00083-2), 2002.
- 689 Herrmann, H., Schaefer, T., Tilgner, A., Styler, S. A., Weller, C., Teich, M., and Otto, T.: Tropospheric aqueous-
690 phase chemistry: Kinetics, mechanisms, and its coupling to a changing gas phase, *Chem. Rev.*, 115, 4259-4334,
691 [10.1021/cr500447k](https://doi.org/10.1021/cr500447k), 2015.
- 692 Hoffmann, M. R.: On the kinetics and mechanism of oxidation of aquated sulfur dioxide by ozone, *Atmos.*
693 *Environ.*, 20, 1145-1154, [10.1016/0004-6981\(86\)90147-2](https://doi.org/10.1016/0004-6981(86)90147-2), 1986.
- 694 Hu, W., Niu, H., Murata, K., Wu, Z., Hu, M., Kojima, T., and Zhang, D.: Bacteria in atmospheric waters: Detection,
695 characteristics and implications, *Atmos. Environ.*, 179, 201-221, <https://doi.org/10.1016/j.atmosenv.2018.02.026>,
696 2018.
- 697 Hutchings, J., Robinson, M., McIlwraith, H., Triplett Kingston, J., and Herckes, P.: The chemistry of intercepted
698 clouds in Northern Arizona during the North American monsoon season, *Water, Air, and Soil Poll.*, 199, 191-202,
699 [10.1007/s11270-008-9871-0](https://doi.org/10.1007/s11270-008-9871-0), 2009.
- 700 Joly, M., Amato, P., Deguillaume, L., Monier, M., Hoose, C., and Delort, A. M.: Quantification of ice nuclei active
701 at near 0 °C temperatures in low-altitude clouds at the Puy de Dôme atmospheric station, *Atmos. Chem. Phys.*, 14,
702 8185-8195, [10.5194/acp-14-8185-2014](https://doi.org/10.5194/acp-14-8185-2014), 2014.
- 703 Kagawa, M., Katsuta, N., and Ishizaka, Y.: Chemical characteristics of cloud water and sulfate production under
704 excess hydrogen peroxide in a high mountainous region of central Japan, *Water, Air, & Soil Pollution*, 232, 177,
705 [10.1007/s11270-021-05099-y](https://doi.org/10.1007/s11270-021-05099-y), 2021.
- 706 Krusiz, C., Berner, A., and Brandner, B.: A cloud water sampler for high wind speeds, *Proceedings of the*
707 *EUROTRAC Symposium 1992* SPB Academic Publishing bv, 1993, 523-525,
- 708 Lamkaddam, H., Dommen, J., Ranjithkumar, A., Gordon, H., Wehrle, G., Krechmer, J., Majluf, F., Salionov, D.,
709 Schmale, J., Bjelić, S., Carslaw, K. S., El Haddad, I., and Baltensperger, U.: Large contribution to secondary
710 organic aerosol from isoprene cloud chemistry, *Science Advances*, 7, eabe2952, [doi:10.1126/sciadv.abe2952](https://doi.org/10.1126/sciadv.abe2952),
711 2021.
- 712 Laskin, A., Laskin, J., and Nizkorodov, S. A.: Chemistry of atmospheric brown carbon, *Chem. Rev.*, 115, 4335-
713 4382, [10.1021/cr5006167](https://doi.org/10.1021/cr5006167), 2015.
- 714 Lawrence, C. E., Casson, P., Brandt, R., Schwab, J. J., Dukett, J. E., Snyder, P., Yergler, E., Kelting, D.,
715 VandenBoer, T. C., and Lance, S.: Long-term monitoring of cloud water chemistry at Whiteface Mountain: the
716 emergence of a new chemical regime, *Atmos. Chem. Phys.*, 23, 1619-1639, [10.5194/acp-23-1619-2023](https://doi.org/10.5194/acp-23-1619-2023), 2023.



- 717 Lebedev, A. T., Polyakova, O. V., Mazur, D. M., Artaev, V. B., Canet, I., Lallement, A., Vaïtilingom, M.,
718 Deguillaume, L., and Delort, A. M.: Detection of semi-volatile compounds in cloud waters by GC×GC-TOF-MS.
719 Evidence of phenols and phthalates as priority pollutants, *Environ. Poll.*, 241, 616-625,
720 <https://doi.org/10.1016/j.envpol.2018.05.089>, 2018.
- 721 Li, J., Wang, X., Chen, J., Zhu, C., Li, W., Li, C., Liu, L., Xu, C., Wen, L., Xue, L., Wang, W., Ding, A., and
722 Herrmann, H.: Chemical composition and droplet size distribution of cloud at the summit of Mount Tai, China,
723 *Atmos. Chem. Phys.*, 17, 9885-9896, 10.5194/acp-17-9885-2017, 2017.
- 724 Li, P. H., Wang, Y., Li, Y.-H., Wang, Z. F., Zhang, H. Y., Xu, P. J., and Wang, W. X.: Characterization of
725 polycyclic aromatic hydrocarbons deposition in PM_{2.5} and cloud/fog water at Mount Taishan (China), *Atmos.*
726 *Environ.*, 44, 1996-2003, 10.1016/j.atmosenv.2010.02.031, 2010.
- 727 Li, T., Wang, Z., Wang, Y., Wu, C., Liang, Y., Xia, M., Yu, C., Yun, H., Wang, W., Wang, Y., Guo, J., Herrmann,
728 H., and Wang, T.: Chemical characteristics of cloud water and the impacts on aerosol properties at a subtropical
729 mountain site in Hong Kong SAR, *Atmos. Chem. Phys.*, 20, 391-407, 10.5194/acp-20-391-2020, 2020.
- 730 Liu, Y., Lim, C. K., Shen, Z., Lee, P. K. H., and Nah, T.: Effects of pH and light exposure on the survival of
731 bacteria and their ability to biodegrade organic compounds in clouds: implications for microbial activity in acidic
732 cloud water, *Atmos. Chem. Phys.*, 23, 1731-1747, 10.5194/acp-23-1731-2023, 2023.
- 733 Löflund, M., Kasper-Giebl, A., Schuster, B., Giebl, H., Hitzenberger, R., and Puxbaum, H.: Formic, acetic, oxalic,
734 malonic and succinic acid concentrations and their contribution to organic carbon in cloud water, *Atmos. Environ.*,
735 36, 1553-1558, 10.1016/s1352-2310(01)00573-8, 2002.
- 736 Lüttke, J., Levsen, K., Acker, K., Wieprecht, W., and Möller, D.: Phenols and nitrated phenols in clouds at mount
737 Brocken, *International Journal of Environ. Anal. Chem.*, 74, 69-89, 10.1080/03067319908031417, 1999.
- 738 MacDonald, A. B., Dadashazar, H., Chuang, P. Y., Crosbie, E., Wang, H., Wang, Z., Jonsson, H. H., Flagan, R.
739 C., Seinfeld, J. H., and Sorooshian, A.: Characteristic vertical profiles of cloud water composition in marine
740 stratocumulus clouds and relationships with precipitation, *Journal of Geophys. Res.: Atmos.*, 123, 3704-3723,
741 <https://doi.org/10.1002/2017JD027900>, 2018.
- 742 Marinoni, A., Laj, P., Sellegri, K., and Mailhot, G.: Cloud chemistry at the puy de Dôme: variability and
743 relationships with environmental factors, *Atmos. Chem. Phys.*, 4, 715-728, 10.5194/acp-4-715-2004, 2004.
- 744 Marinoni, A., Parazols, M., Brigante, M., Deguillaume, L., Amato, P., Delort, A.-M., Laj, P., and Mailhot, G.:
745 Hydrogen peroxide in natural cloud water: Sources and photoreactivity, *Atmos. Res.*, 101, 256-263,
746 10.1016/j.atmosres.2011.02.013, 2011.
- 747 Marple, V. A. and Willeke, K.: Impactor design, *Atmos. Environ.* (1967), 10, 891-896,
748 [https://doi.org/10.1016/0004-6981\(76\)90144-X](https://doi.org/10.1016/0004-6981(76)90144-X), 1976.
- 749 Munger, J. W., Jacob, D. J., Waldman, J. M., and Hoffmann, M. R.: Fogwater chemistry in an urban atmosphere,
750 *Journal of Geophys. Res.*, 88, 5109-5121, <https://doi.org/10.1029/JC088iC09p05109>, 1983.
- 751 Munger, J. W., Jacob, D. J., Daube, B. C., Horowitz, L. W., Keene, W. C., and Heikes, B. G.: Formaldehyde,
752 glyoxal, and methylglyoxal in air and cloudwater at a rural mountain site in central Virginia, *Journal of Geophys.*
753 *Res.*, 100, 9325-9333, 10.1029/95jd00508, 1995.
- 754 Pailler, L., Wirgot, N., Joly, M., Renard, P., Mouchel-Vallon, C., Bianco, A., Leriche, M., Sancelme, M., Job, A.,
755 Patryl, L., Armand, P., Delort, A.-M., Chaumerliac, N., and Deguillaume, L.: Assessing the efficiency of water-



- 756 soluble organic compound biodegradation in clouds under various environmental conditions, *Environ. Sci.:*
757 *Atmos.*, 3, 731-748, 10.1039/D2EA00153E, 2023.
- 758 Pye, H. O. T., Nenes, A., Alexander, B., Ault, A. P., Barth, M. C., Clegg, S. L., Collett Jr, J. L., Fahey, K. M.,
759 Hennigan, C. J., Herrmann, H., Kanakidou, M., Kelly, J. T., Ku, I. T., McNeill, V. F., Riemer, N., Schaefer, T.,
760 Shi, G., Tilgner, A., Walker, J. T., Wang, T., Weber, R., Xing, J., Zaveri, R. A., and Zuend, A.: The acidity of
761 atmospheric particles and clouds, *Atmos. Chem. Phys.*, 20, 4809-4888, 10.5194/acp-20-4809-2020, 2020.
- 762 Renard, P., Bianco, A., Baray, J.-L., Bridoux, M., Delort, A.-M., and Deguillaume, L.: Classification of clouds
763 sampled at the puy de Dôme station (France) based on chemical measurements and air mass history matrices,
764 *Atmosphere*, 11, 732, <https://doi.org/10.3390/atmos11070732>, 2020.
- 765 Renard, P., Brissy, M., Rossi, F., Lereboure, M., Jaber, S., Baray, J. L., Bianco, A., Delort, A. M., and
766 Deguillaume, L.: Free amino acid quantification in cloud water at the Puy de Dôme station (France), *Atmos. Chem.*
767 *Phys.*, 22, 2467-2486, 10.5194/acp-22-2467-2022, 2022.
- 768 Roman, P., Polkowska, Ż., and Namieśnik, J.: Sampling procedures in studies of cloud water composition: a
769 review, *Critical Reviews in Environmental Science and Technology*, 43, 1517-1555,
770 10.1080/10643389.2011.647794, 2013.
- 771 Rossi, F., Péguilhan, R., Turgeon, N., Veillette, M., Baray, J.-L., Deguillaume, L., Amato, P., and Duchaine, C.:
772 Quantification of antibiotic resistance genes (ARGs) in clouds at a mountain site (puy de Dôme, central France),
773 *STOTEN*, 865, 161264, <https://doi.org/10.1016/j.scitotenv.2022.161264>, 2023.
- 774 Schell, D., Georgii, H. W., Maser, R., Jaeschke, W., Arends, B. G., Kos, G. P. A., Winkler, P., Schneider, T.,
775 Berner, A., and Krusisz, C.: Intercomparison of fog water samplers, *Tellus B*, 44, 612-631,
776 <https://doi.org/10.1034/j.1600-0889.1992.t01-1-00014.x>, 1992.
- 777 Schurman, M. I., Boris, A., Desyaterik, Y., and Collett, J. J. L.: Aqueous secondary organic aerosol formation in
778 ambient cloud water photo-oxidations, *AAQR*, 18, 15-25, 10.4209/aaqr.2017.01.0029, 2018.
- 779 Skarżyńska, K., Polkowska, Ż., and Namieśnik, J.: Sampling of atmospheric precipitation and deposits for analysis
780 of atmospheric pollution, *Journal of Automated Methods and Management in Chemistry*, 2006, 026908,
781 10.1155/JAMMC/2006/26908, 2006.
- 782 Sun, W., Fu, Y., Zhang, G., Yang, Y., Jiang, F., Lian, X., Jiang, B., Liao, Y., Bi, X., Chen, D., Chen, J., Wang, X.,
783 Ou, J., Peng, P., and Sheng, G.: Measurement report: Molecular characteristics of cloud water in southern China
784 and insights into aqueous-phase processes from Fourier transform ion cyclotron resonance mass spectrometry,
785 *Atmos. Chem. Phys.*, 21, 16631-16644, 10.5194/acp-21-16631-2021, 2021.
- 786 Sun, X., Wang, Y., Li, H., Yang, X., Sun, L., Wang, X., Wang, T., and Wang, W.: Organic acids in cloud water
787 and rainwater at a mountain site in acid rain areas of South China, *Environmental Science and Pollution Research*,
788 23, 9529-9539, 10.1007/s11356-016-6038-1, 2016.
- 789 Tenberken-Pötzsch, B., Schwikowski, M., and Gäggeler, H. W.: A method to sample and separate ice crystals and
790 supercooled cloud droplets in mixed phased clouds for subsequent chemical analysis, *Atmos. Environ.*, 34, 3629-
791 3633, [https://doi.org/10.1016/S1352-2310\(00\)00140-0](https://doi.org/10.1016/S1352-2310(00)00140-0), 2000.
- 792 Triesch, N., van Pinxteren, M., Engel, A., and Herrmann, H.: Concerted measurements of free amino acids at the
793 Cape Verde Islands: High enrichments in submicron sea spray aerosol particles and cloud droplets, *Atmos. Chem.*
794 *Phys.*, 21, 163-181, 10.5194/acp-21-163-2021, 2021.



- 795 Vaitilingom, M., Deguillaume, L., Vinatier, V., Sancelme, M., Amato, P., Chaumerliac, N., and Delort, A.-M.:
796 Potential impact of microbial activity on the oxidant capacity and organic carbon budget in clouds, *PNAS*, 110,
797 559-564, 10.1073/pnas.1205743110, 2013.
- 798 Vaitilingom, M., Attard, E., Gaiani, N., Sancelme, M., Deguillaume, L., Flossmann, A. I., Amato, P., and Delort,
799 A.-M.: Long-term features of cloud microbiology at the puy de Dôme (France), *Atmos. Environ.*, 56, 88-100,
800 10.1016/j.atmosenv.2012.03.072, 2012.
- 801 van Pinxteren, D., Neusüß, C., and Herrmann, H.: On the abundance and source contributions of dicarboxylic acids
802 in size-resolved aerosol particles at continental sites in central Europe, *Atmos. Chem. Phys.*, 14, 3913-3928,
803 10.5194/acp-14-3913-2014, 2014.
- 804 van Pinxteren, D., Fomba, K. W., Mertes, S., Müller, K., Spindler, G., Schneider, J., Lee, T., Collett, J. L., and
805 Herrmann, H.: Cloud water composition during HCCT-2010: Scavenging efficiencies, solute concentrations, and
806 droplet size dependence of inorganic ions and dissolved organic carbon, *Atmos. Chem. Phys.*, 16, 3185-3205,
807 10.5194/acp-16-3185-2016, 2016.
- 808 van Pinxteren, D., Plewka, A., Hofmann, D., Müller, K., Kramberger, H., Svcina, B., Bächmann, K., Jaeschke,
809 W., Mertes, S., Collett Jr, J. L., and Herrmann, H.: Schmücke hill cap cloud and valley stations aerosol
810 characterisation during FEBUKO (II): Organic compounds, *Atmos. Environ.*, 39, 4305-4320,
811 10.1016/j.atmosenv.2005.02.014, 2005.
- 812 van Pinxteren, M., Fomba, K. W., Triesch, N., Stolle, C., Wurl, O., Bahlmann, E., Gong, X., Voigtländer, J., Wex,
813 H., Robinson, T. B., Barthel, S., Zeppenfeld, S., Hoffmann, E. H., Roveretto, M., Li, C., Grosselin, B., Daële, V.,
814 Senf, F., van Pinxteren, D., Manzi, M., Zabalegui, N., Frka, S., Gašparović, B., Pereira, R., Li, T., Wen, L., Li, J.,
815 Zhu, C., Chen, H., Chen, J., Fiedler, B., von Tümpling, W., Read, K. A., Punjabi, S., Lewis, A. C., Hopkins, J. R.,
816 Carpenter, L. J., Peeken, I., Rixen, T., Schulz-Bull, D., Monge, M. E., Mellouki, A., George, C., Stratmann, F.,
817 and Herrmann, H.: Marine organic matter in the remote environment of the Cape Verde islands – an introduction
818 and overview to the MarParCloud campaign, *Atmos. Chem. Phys.*, 20, 6921-6951, 10.5194/acp-20-6921-2020,
819 2020.
- 820 Waldman, J. M., Munger, J. W., J., J. D., and Hoffmann, M. R.: Chemical characterization of stratus cloudwater
821 and its role as a vector for pollutant deposition in a Los Angeles pine forest, *Tellus B*, 37B, 91-108,
822 <https://doi.org/10.1111/j.1600-0889.1985.tb00058.x>, 1985.
- 823 Wang, M., Perroux, H., Fleuret, J., Bianco, A., Bouvier, L., Colomb, A., Borbon, A., and Deguillaume, L.:
824 Anthropogenic and biogenic hydrophobic VOCs detected in clouds at the puy de Dôme station using Stir Bar
825 Sorptive Extraction: Deviation from the Henry's law prediction, *Atmos. Res.*, 237, 104844,
826 <https://doi.org/10.1016/j.atmosres.2020.104844>, 2020.
- 827 Wei, M., Xu, C., Chen, J., Zhu, C., Li, J., and Lv, G.: Characteristics of bacterial community in cloud water at Mt
828 Tai: similarity and disparity under polluted and non-polluted cloud episodes, *Atmos. Chem. Phys.*, 17, 5253-5270,
829 10.5194/acp-17-5253-2017, 2017.
- 830 Wieprecht, W., Acker, K., Mertes, S., Collett, J., Jaeschke, W., Brüggemann, E., Möller, D., and Herrmann, H.:
831 Cloud physics and cloud water sampler comparison during FEBUKO, *Atmos. Environ.*, 39, 4267-4277,
832 <https://doi.org/10.1016/j.atmosenv.2005.02.012>, 2005.



- 833 Wright, L. P., Zhang, L., Cheng, I., Aherne, J., and Wentworth, G. R.: Impacts and effects indicators of
834 atmospheric deposition of major pollutants to various ecosystems - a review, AAQR, 18, 1953-1992,
835 10.4209/aaqr.2018.03.0107, 2018.
- 836 Xu, C., Wei, M., Chen, J., Sui, X., Zhu, C., Li, J., Zheng, L., Sui, G., Li, W., Wang, W., Zhang, Q., and Mellouki,
837 A.: Investigation of diverse bacteria in cloud water at Mt. Tai, China, STOTEN, 580, 258-265,
838 <http://dx.doi.org/10.1016/j.scitotenv.2016.12.081>, 2017.
- 839 Zhao, Y., Hallar, A. G., and Mazzoleni, L. R.: Atmospheric organic matter in clouds: exact masses and molecular
840 formula identification using ultrahigh-resolution FT-ICR mass spectrometry, Atmos. Chem. Phys., 13, 12343-
841 12362, 10.5194/acp-13-12343-2013, 2013.